

# Evidence for interchange reconnection between a coronal hole and an adjacent emerging flux region

D. Baker<sup>1,\*</sup>, L. van Driel-Gesztelyi<sup>1,2,3</sup>, and G. D. R. Attrill<sup>1</sup>

<sup>1</sup> Mullard Space Science Laboratory, University College London, Holmbury St. Mary, Dorking, Surrey, RH5 6NT, UK

<sup>2</sup> Observatoire de Paris, LESIA, 92195 Meudon Cedex, France

<sup>3</sup> Konkoly Observatory of the Hungarian Academy of Sciences, P.O. Box 67, H-1525, Budapest, Hungary

Received 15 Mar 2007, accepted 23 Apr 2007

Published online later

**Key words** Sun: coronal active regions – Sun: coronal holes – Sun: magnetic fields – Sun: magnetic reconnection

Coronal holes are regions of dominantly monopolar magnetic field on the Sun where the field is considered to be 'open' towards interplanetary space. Magnetic bipoles emerging in proximity to a coronal hole boundary naturally interact with this surrounding open magnetic field. In the case of oppositely aligned polarities between the active region and the coronal hole, we expect interchange reconnection to take place, driven by the coronal expansion of the emerging bipole as well as occasional eruptive events. Using SOHO/EIT and SOHO/MDI data, we present observational evidence of such interchange reconnection by studying AR 10869 which emerged close to a coronal hole. We find closed loops forming between the active region and the coronal hole leading to the retreat of the hole. At the same time, on the far side of the active region, we see dimming of the corona which we interpret as a signature of field line 'opening' there, as a consequence of a topological displacement of the 'open' field lines of the coronal hole.

© 2006 WILEY-VCH Verlag GmbH & Co. KGaA, Weinheim

## 1 Introduction

The magnetic field on the Sun's surface is inhomogeneous and complex. It is distributed in numerous structures of varying sizes and strengths. Quiet sun (QS) is found over most of the solar surface and is characterized by small scale mixed polarities. Active regions (ARs) typically emerge with a bipolar structure containing roughly equal quantities of positive and negative magnetic flux. Emerging bipoles either make up a component of the quiet sun or become ARs if they are larger than 2.5 heliographic degrees<sup>2</sup> (Hagenaar *et al.* 2003). Small ARs have lifetimes of days to weeks and magnetic flux of  $1 \times 10^{20}$  Mx to  $5 \times 10^{21}$  Mx. Large ARs have lifetimes of the order of a few months and magnetic flux at maximum development of  $5 \times 10^{21}$  Mx to  $4 \times 10^{22}$  Mx (Zwaan 1987).

Because of the nature of bipolar ARs, loop structures of closed field lines are created. Coronal loops are filled with plasma of temperatures over  $10^6$  K. These loops are hotter and denser than the background corona and produce bright emission in the extreme ultraviolet and soft X-ray ranges.

Whereas ARs contain mainly closed magnetic field lines, coronal holes (CHs) are regions of low emission dominated by 'open' magnetic field lines. Plasma is evacuated into interplanetary space along the 'open' field lines, therefore, CHs provide the source for high-speed particle streams or the fast solar wind.

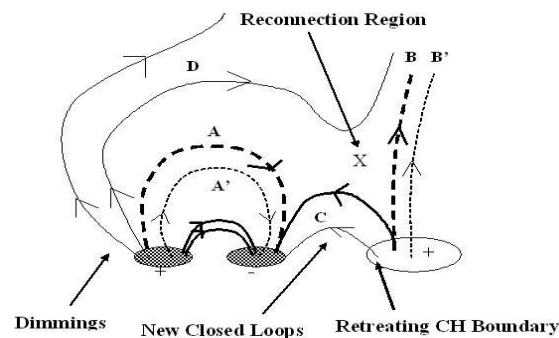


**Fig. 1** Sketch of magnetic field configuration favorable for interchange reconnection. AR polarities are shown with hash regions on the left. Dashed (solid) lines represent pre (post)-reconnection configuration. AR's expanding loops marked by **A** reconnect with oppositely oriented open CH field lines marked by **B**. New closed loops are formed at **C** and field lines are 'opened' at **D** as reconnection proceeds. (**A'** reconnects with **B'** and so on.)

The low emission of CHs is due to lower electron density and temperature, consequently, they appear darker than the QS when observed in EUV emission lines. Typically, CHs are detected in EUV Fe emission lines, SXR emission, radio emission and He I and He II lines (de Toma & Arge 2005; van Driel-Gesztelyi 2006). However, CHs can have different extents when observed at different wavelengths (de Toma & Arge 2005). This poses a problem for identifying CH boundaries.

The emergence and growth of ARs force topological changes in the magnetic field of the overlying and surround-

\* Corresponding author: e-mail: db2@mssl.ucl.ac.uk

ing corona. Magnetic reconnection may occur depending on the relative orientation of the AR's field and that of the neighbouring fields. Specifically, we expect that oppositely oriented components of closed field lines of an AR and 'open' field lines of a nearby CH can provide the magnetic field configuration required for interchange reconnection (Crooker *et al.* 2002), which displaces 'open' field lines in a step-wise manner while conserving the amount of field lines open towards the interplanetary space (Fisk 2005).

If a CH exists near an AR, then expansion of the AR can push the closed field lines against the 'open' field lines of the nearby CH. At the interface of the oppositely oriented magnetic field components, a current sheet may form leading to magnetic reconnection. We sketch in Figure 1 the expected scenario: the expanding magnetic loops of the AR (A) reconnect at (X) with the 'open' field lines of the nearby CH (B). After reconnection, new closed loops are formed which connect the negative polarity of the AR and the positive CH field (C). Here, reconnection of successive field lines closes down the CH field making the boundary retreat as the CH shrinks. As well as creating bright closed loops, reconnection 'opens' field lines on the left of the AR (D). Plasma no longer trapped in the closed AR loops is evacuated along the 'open' field lines into the heliosphere (Hudson, Acton, & Freeland 1996), leading to dimming of the coronal brightness.

Interchange reconnection may have important implications for the evolution of CHs as well as for the eruptive activity of ARs. ARs have been observed expanding into the outer corona at speeds of a few  $10 \text{ km s}^{-1}$  to  $100 \text{ km s}^{-1}$  (Uchida *et al.* 1992). Higher velocities are related to eruptive events such as coronal mass ejections. We expect ARs within or on the boundary of CHs to be more eruptive since interchange reconnection naturally removes overlying field lines that stabilize potentially eruptive AR filaments/flux ropes.

Attrill *et al.* (2006) provided evidence for interchange reconnection happening in a similar scenario as that described in Figure 1 but forced by the expansion of a CME. Here we are looking for evidence of interchange reconnection during the flux emergence phase of an AR adjacent to a CH.

## 2 Active Region NOAA 10869

AR 10869, located  $\approx 200''$  east of an extension of the south polar CH, started to emerge at 01:35 UT on 5 April 2006 as a magnetic bipole oriented in an east-west direction. The new flux emergence occurred in the eastern hemisphere just south of the solar equator. At maximum development, magnetic flux was measured to be  $2.3 \times 10^{21} \text{ Mx}$ . This peak flux puts AR 10869 in the 'small' AR category. The negative (leading) polarity of the AR was in close proximity to the positive polarity of the CH, thus, AR 10869 is ideal for observing possible signatures of interchange reconnection.

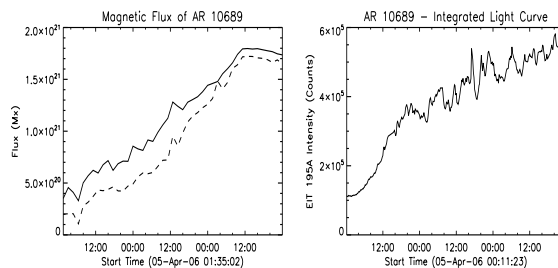


**Fig. 2** Left panel - Magnetic flux evolution of AR 10869. Positive/negative (continuous/dashed) curves are shown. Right panel - Light curve showing temporal variation in EUV intensity of AR 10869.

## 3 Data Analysis

This study of AR10869 uses full-disk level 1.8 SOHO/MDI (Scherrer *et al.* 1995) magnetograms with 96 min time cadence and a pixel size of  $1.98''$ . The data were corrected for geometrical distortions using the standard `zradialize` routine in SolarSoft. MDI full-disk calibration underestimates magnetic flux density (Berger & Lites 2003), therefore, the data were corrected for both linear and non-linear response using  $\Phi_{corrected} = 1.45(\Phi + 0.3\Phi_{B>1200G})$  (Green *et al.* 2003). Magnetic flux was obtained by fitting a contour defined by eye around the boundary of the AR, limiting the contribution of the unrelated background field. Flux was summed within this region on each magnetogram.

SOHO/EIT (Delaboudinière *et al.* 1995)  $195\text{\AA} \approx 12 \text{ min}$  high cadence, full-disk images are used to analyze the evolution of AR 10869. All MDI and EIT images were derotated to the same time (12:47 UT on 5 April 2006). Base difference images where the same pre-emergence image (21:59 UT 4 April 2006) is subtracted from all images in the series were used to accentuate the evolving features of the AR. The CH boundary was defined as the intensity level halfway between the intensity levels of the south polar CH and a region of quiet sun (as in Attrill *et al.* 2006). The boundary was overlaid on the EIT images.

The data series runs from 00:11 UT on 5 April 2006 to 23:47 UT on 7 April 2006.

## 4 Results and Discussion

### 4.1 Magnetic flux evolution

Figure 2 shows the total flux ( $B \geq 10 \text{ G}$ ) of AR 10869. The positive (solid line) and negative (dashed line) fluxes are imbalanced with the following polarity (positive) dominating when AR 10869 is in the eastern hemisphere. There are two sources of this imbalance. First, the quiet sun around the AR is dominantly positive and makes up more of the total flux within the contour region during early emergence. Second, the presence of a horizontal magnetic field component gives a stronger contribution to the line-of-sight flux of AR 10869 when it is further away from the solar central meridian (Green *et al.* 2003). The following positive polarity is

located further away from the central meridian thus its horizontal field component contribution is greater compared to that of the leading polarity. Imbalance of positive over negative flux decreases as the region moves closer to the central meridian.

The integrated light curve of the AR EUV emission at 195 Å is shown in the *right panel* of Figure 2. A comparison of the curves shown in the two panels reveals an expected correlation between the increases in magnetic flux and intensity as the AR expands and evolves.

The magnetic evolution over time is shown in Figure 3 (1st column). At first, individual bipoles appear with no definite neutral line. As the flux tube emerges, there is a coalescence of the flux elements after a few hours which can be seen in the 1st frame of MDI images shown. By the 2nd frame, the flux elements are organized into distinct polarities with a single magnetic inversion line. As surface area increases so does the magnetic flux of both polarities. Opposite polarities have separated in the last frame. This progression of AR development is consistent with the birth and evolution of emerging regions described in van Driel-Gesztelyi (2002, and references therein).

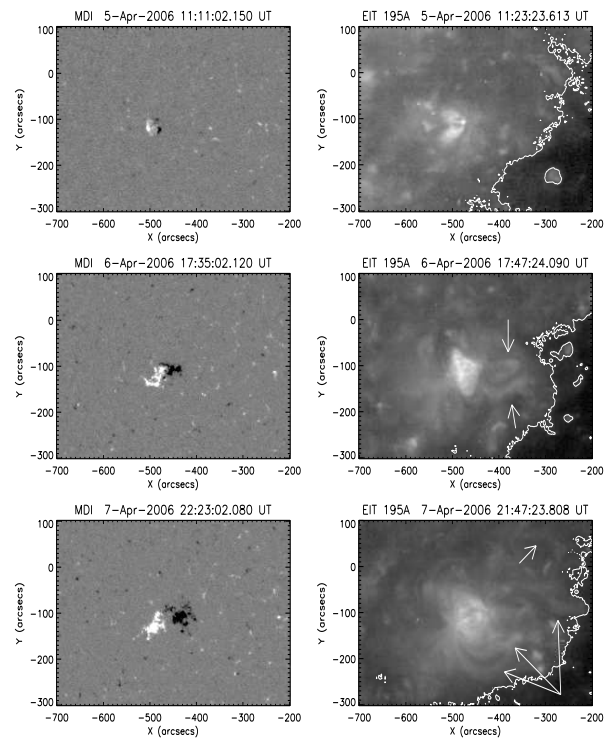
#### 4.2 Observed signatures of interchange reconnection

Figure 3, 2nd column, contains a series of EIT 195 Å images showing the expansion of the AR and its interaction with the CH. The white contour shows the CH boundary.

Early on, the AR is small surrounded by short, bright loops extending in all directions (see 1st image). By the 2nd image, the AR is expanding and new bright loops (indicated by the white arrows) are forming towards the CH boundary. Increases of magnetic flux and area can be seen in the corresponding MDI magnetogram. An extensive system of new loops can be observed towards the west and southwest in the 3rd image. By this time, virtually all of the new closed loops are forming in the direction of the CH. Concurrently, the CH boundary is receding as the CH field is closed down by reconnection (see Figure 1). The boundary retreats  $\approx 30''$  directly to the west of the AR core and  $\approx 60''$  to the southwest.

These observational signatures are evident in Figure 4 in the 2-D stack plot of intensity along an east-west slice from the far side of the AR to inside the CH. The AR core expansion, new closed loops formation and CH boundary retreat are indicated in the figure.

Light curves of regions around AR 10869 present further evidence of interchange reconnection signatures. Figure 5, *left panel*, consists of two EIT 195 Å images overlaid with contours defining the expected eastern dimming and western new loops regions. The top image shows an early stage of evolution when the AR is relatively small. Initially, both contour regions avoid encroaching AR core light contamination. By the time of the bottom image (7 April 2006 16:59 UT), the AR has expanded and moved into the western contour which means an integrated light curve will include light from the bright core. A second western contour



**Fig. 3** *Left panel* - SOHO/MDI images of AR 10869's photospheric magnetic field evolution. White (black) is positive (negative) polarity. *Right panel* - SOHO/EIT 195 Å images of AR 10869 and a nearby CH to the west (right in the images). Overlaid is the CH boundary shown in white. The boundary is defined as the intensity level half way between that of the southern polar CH and quiet sun.

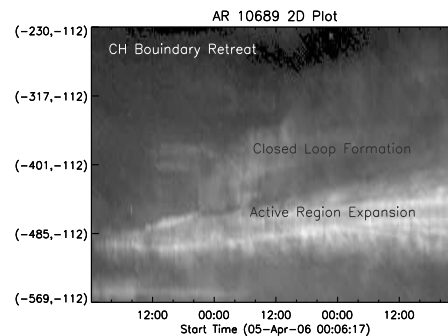


**Fig. 4** EUV intensity stack plot along an east-west cut extending from east of AR 10869 to the CH. (Y-axis units are arcsec).

is chosen further away from the AR to avoid this problem. The *right panel* of Figure 5 shows integrated light curves of the contour regions. The truncated solid line is a light curve of the original western contour close to the AR. The curve ends when the AR core is about to move inside the contour. The other solid line is the light curve for the second western contour which avoids core light contamination at the expense of capturing early closed loop formation. Finally, the dashed line is the light curve of the far side of the

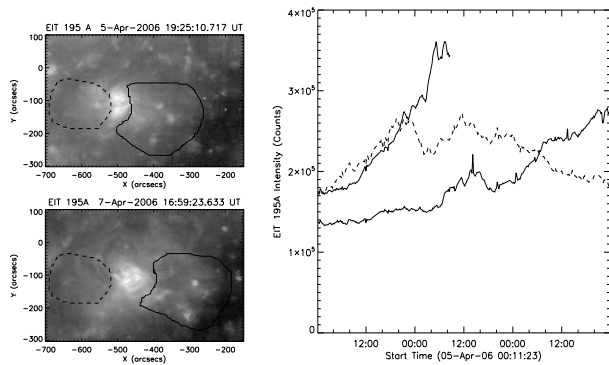


**Fig. 5** *Left panel* - EIT 195 Å images overlaid with selected contour regions to the east and west of AR 10869. (Top) AR is small and both contour regions avoid AR core light contamination. (Bottom) AR has expanded and moved into the original western contour. A second western contour is selected to avoid core light contamination. *Right panel* - Integrated light curves of dimming region to the east (dashed line), original western contour (top truncated solid line), and second western contour (bottom solid line).

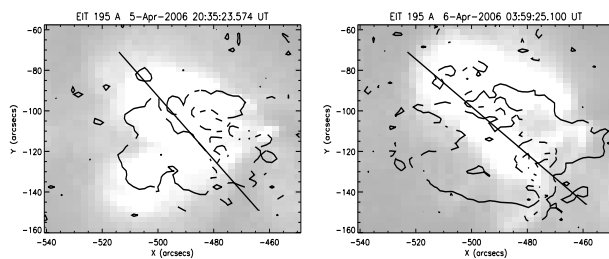


**Fig. 6** SOHO/EIT 195 Å images prior to and during deepest dimming (see Figure 5) overlaid with magnetic field contours. Magnetic inversion lines determined by eye are shown. Negative/positive polarity region is to the right/left on the magnetic inversion line.

AR region where dimming is expected. The light curve of this region is not affected by core light because the eastern boundary of the AR does not change significantly.

The top two light curves evolve in a similar manner as the emerging bipole reconnects with pre-existing magnetic structures in the vicinity of the AR. Divergence begins at  $\approx 0:00$  UT on 6 April. The original western region light curve shows a sharp increase concurrent with a dimming in the dashed curve. The light curve of the second western contour region does not start to rise for another few hours because this contour excludes intensity from early loop formation. Brightness changes in the western loop formation and the eastern dimming regions continue in opposite directions throughout AR evolution.

Evidence of dimming on the far side of the AR is shown in Figure 6. The figure contains two EIT images overlaid with magnetic field contours and magnetic inversion lines. Magnetic field concentrations  $\geq 20$  G and inversion lines determined by eye are shown. Negative field concentration is indicated by contours to the west (right) of the magnetic inversion lines and positive field concentration is indicated

by contours to the east (left). Bright, closed loops lie almost entirely over both AR polarities prior to the onset of dimming (*left panel*). By 04:00 UT on 6 April, at the time of the deepest dimming, closed AR loops no longer fully cover the positive field (see the ‘empty’ part of the contour) to the east of the AR core (*right panel*). Pre-dimming EIT images show the protruding foot-points were formerly connected by bright EIT loops. Now the foot-points of the dimmed positive polarity region are end-points of newly forming loops on the west side. As the positive magnetic field in the CH is closed down, new positive field is ‘opened’ at the positive polarity of the AR. In addition, the dimming on the far side of the AR occurs during a period of accelerated closed loop formation (Figure 4), possibly caused by a mini-CME, as evidenced by the sharp rise in EUV intensity (Figure 5, truncated curve).

The dimming to the east and the development of the loops to the west appear to be correlated in time. We interpret this to mean we are observing coronal signatures of open field lines which are created during interchange reconnection between the closed field lines of the AR and the ‘open’ field lines of the CH. Taken together these observations provide strong evidence for the emerging active region - coronal hole interaction predicted.

*Acknowledgements.* D.B. and G.D.R.A. thank the British Council for sponsoring the conference and PPARC for support via PhD studentships. LvDG acknowledges Hungarian government grant OTKA T048961. We thank SOHO/EIT and MDI consortia for their data. SOHO is a project of international cooperation between ESA and NASA. The authors are grateful to the anonymous referee, Tibor Török, and Pascal Démoulin for their valuable input.

## References

- Attrill, G., Nakwacki, M.S., Harra, L.K., van Driel-Gesztelyi, L., Dasso, S., Wang, J.: 2006, *Solar Phys.* **238**, 117
- Berger, T.E., Lites, B.W.: 2003, *Solar Phys.* **213**, 213
- Crooker, N.U., Gosling, J.T., Kahler, S.W.: 2002, *J. Geophys. Res.* **107**, 1028
- Delaboudinière, J.-P., Artzner, G.E., Brunaud, J., et al.: 1995, *Solar Phys.* **162**, 291
- de Toma, G., Arge, C.N.: 2005, Large-scale structures and their role in solar activity, ASP Conference Series, Vol. 346, p251
- Fisk, L.A.: 2005, *ApJ.* **626**, 563
- Green, L.M., Démoulin, P., Mandrini, C.H., van Driel-Gesztelyi, L.: 2003, *Solar Phys.* **215**, 307
- Hagenaar, H.J., Schriver, C.J., Title, A.M.: 2003, *ApJ.* **584**, 1107
- Hudson, H.S., Acton, L.W., Freeland, S.L.: 1996, *ApJ.* **470**, 629
- Scherrer, P.H., Bogart, R.S., Bush, R.I., et al.: 1995, *Solar Phys.* **162**, 129
- Uchida, Y., McAllister, A., Strong, K.T., Ogawara, Y., Shimizu, T., Matsumoto, R., Hudson, H.S.: 1992, *PASJ* **44**, L155
- van Driel-Gesztelyi, L.: 2002, SOLMAG 2002, Proc. IAU Coll. 188, ESA SP-505, ISBN 92-9092-815-8, 2002, p113
- van Driel-Gesztelyi, L.: 2006, IAU, 233, Cambridge University Press, 2006, p205
- Zwaan, C.: 1987, *Ann. Rev. Astron. Astrophys.* **25**, 83